Comparison of radiation exposure to the patient and contrast detail resolutions across micro dose 2D/3D slot scanner and two conventional digital radiography X-ray imaging systems

AUTHORS

Ahmed Jibril Abdi, Medical Physicist, MSc [1, *]
Bo Mussmann, Researcher Radiographer PhD[2]
Alistair Mackenzie, Research Physicist MSc, PhD[3]
Benedikte Klaerke, Medical Physicist, PhD[1]
Poul Erik Andersen, professor, head of research, PhD[4]

[1]Region of Southern Denmark, Clinical Engineering Department, Area of Diagnostic Radiology, .B. Winsløws Vej 4, Indgang 34, 5000 Odense C, Denmark,
[2] Department of Radiology, Odense University Hospital, 5000 Odense C, Denmark
[3]National Coordinating Centre for the Physics of Mammography, Royal Surrey County Hospital, Guildford, GU2 7XX, United Kingdom
[4] Department of Clinical Research, University of Southern Denmark, 5000 Odense C, Denmark

* E-mail: ahmed.abdi@rsyd.dk, Phone: +45 20422535

COMPARISON OF RADIATION EXPOSURE TO THE PATIENT AND CONTRAST DETAIL
RESOLUTIONS ACROSS LOW DOSE 2D/3D SLOT SCANNER AND TWO CONVENTIONAL DIGITAL RADIOGRAPHY X-RAY IMAGING SYSTEMS,
Radiation Protection Dosimetry, Volume 185, Issue 2, November 2019, Pages 252–265, https://dx.doi.org/10.1093/rpd/ncz006.

ABSTRACT

Purpose*:* To assess and compare the radiation dose and image quality of the micro dose 2D/3D EOS slot scanner (MDSS) to conventional digital radiography (DR) X-ray imaging systems for chest and knee examination protocols.

Methods and materials: The effective doses (ED) to the patient in the chest and knee clinical examination protocols for MDSS and DR X-ray imaging systems were determined using the dose area product and PCXMC Monte Carlo simulation software. The CDRAD phantom was imaged with 19 cm, and 13 cm thick Polymethyl Methacrylate (PMMA) blocks to simulate the chest and knees respectively of a patient of average adult size. The contrast detail resolution was calculated using image analysis software.

Results: The EDs for the MDSS default setting were up to 69% and 51% lower than for the DR systems for the chest (speed 4s) and knee (speed 6s) protocols respectively, while for the increased dose level setting then the EDs were up to 42% and 35% lower than for the DR systems for the chest (speed 6s) and knee (speed 8s) protocols respectively. At the default setting the contrast detail was lowest for the default setting of the 2D/3D micro dose slot scanner (MDSS) for both chest and knee examinations, but at the highest dose levels then the threshold were equal or higher than the contrast resolution of DR imaging systems.

Conclusion: The MDSS has the potential to be used for clinical diagnosis of chest and knee examinations using the higher dose level. For speed 6s in chest protocol and speed 8s in knee protocol, the measured contrast detail resolution was comparable with the DR systems but at a lower effective dose.

1. INTRODUCTION

The number of X-ray examinations has been increasing over the last decades [1,2]. Also, X-ray imaging systems have been improved in order to minimise radiation exposure to the patients while maintaining sufficient clinical image quality. The micro dose 2D/3D slot scanner (MDSS) is a relatively new X-ray imaging system that produces two-dimensional (2D) X-ray images similar to those derived by conventional radiography imaging systems [3,4]. However, this system differs from conventional systems in that it uses slot-scan technology, which means the system scans one line at a time rather than capturing the entire image from a single exposure. The system vertically scans the entire or a single part of the body, with the patient in a weight-bearing position. The MDSS imaging system takes simultaneous images in two planes (posterior-anterior and lateral). By using a computer algorithm, the system can construct three-dimensional (3D) surface images from the simultaneous two-plane images [5,6]. The MDSS is designed to lower patient doses compared with conventional digital radiography (DR) X-ray imaging systems and a few studies have shown substantial clinical potential for dose savings compared to DR and computed radiography (CR) [7–12]. The MDSS X-ray imaging system is mainly used to obtain overview images in patients with scoliosis and to measure the length of lower extremities. To our knowledge, the MDSS X-ray imaging system is currently not used for diagnostic X-ray examinations, as comprehensive studies to determine whether this system can be used for other anatomical regions have not been undertaken. There is an indication that the MDSS imaging system has a potential for use as a conventional radiographic imaging system [13]. It has also been shown that the image quality of the MDSS imaging system is comparable to that of conventional DR imaging systems for the clinical spine protocol [14]. More comprehensive research and investigations are needed to assess if the MDSS imaging system can substitute clinical X-ray examinations for other anatomical regions[11,15].

The purpose of the study was to assess the radiation dose in chest and extremities protocols using the MDSS imaging system compared to two DR systems. Contrast detail resolution is a useful parameter and objective method for evaluating the overall image quality of X-ray imaging systems. The radiological image of the CDRAD test object can also be scored subjectively by observers [16,17] or using automatic scoring software [18]. To investigate whether the MDSS X-ray imaging system can be used in clinical practice for X-ray imaging examinations, the image quality of the MDSS was evaluated objectively and compared to the results of examinations of thorax and extremity regions using conventional DR X-ray imaging systems.

2. MATERIALS AND METHODS

The following equipment and tools were used to assess radiation exposure to the patient and to determine the contrast detail resolutions of different clinical examination settings in MDSS imaging system and two conventional DR X-ray imaging systems. The image quality (contrast detail resolution) and radiation exposure of the systems were then evaluated and compared.

2.1 Imaging systems

The MDSS imaging system (EOS SA, Paris, FRANCE) (www.eos-imaging.com) allows the acquisition of two simultaneous X-rays images, which are the posterior-anterior and lateral projections. Using these two-dimensional (2D) images, it is possible to derive three-dimensional (3D) model images for angulation and distance measurements. It is also possible to activate only one source of the system to acquire a 2D image. When the two sources of the system are activated, the MDSS system is comparable to a conventional biplane radiological imaging system. The system also has two 1 mm thick gaseous X-ray detectors, which are placed perpendicular to each other in the PA and lateral positions[19].

Two conventional DR X-ray systems were used for comparison:

- DR system 1: Philips Digital Diagnost (DiDi) DR X-ray imaging system (Philips Healthcare, Best, Netherlands) with a Trixell flat panel wall stand detector.
- DR system 2: Siemens Ysio DR X-ray imaging system (Siemens Healthineers GmbH, Forchheim, Germany) with a Trixell flat panel wall stand receptor

2.2 Phantoms

A 40 cm x 40 cm, 18 cm thick block of Polymethyl Methacrylate (PMMA) was used, with the addition of a 1 cm thick CDRAD test object (in total 19 cm thick PMMA attenuation plates), which corresponds to the typical patient with average adult thickness was used for the chest protocol [20]. To simulate the attenuation in a typical extremity examination, a 12 cm thick PMMA block plus 1 cm of CDRAD PMMA test object (13 cm in total) was used for knee protocol [21].

The chest and neck part of Alderson phantom (Radiology Support devices (RSD), Alderson phantoms, Long Beach, CA 90810 USA) was used to measure the organ doses directly in the chest examination protocol. This Alderson anthropomorphic phantom is suitable for measuring doses for specific organs in a human body exposed during a diagnostic X-ray examination.

The contrast detail resolution of the systems was evaluated using the CDRAD phantom (Artinis medical systems B.V, Elst, The Netherlands). The CDRAD contrast detail test object is a PMMA attenuation plate with dimensions of 26.5 cm × 26.5 cm × 1.0 cm, and contains 225 squares, 15 rows and 15 columns. The squares of the top three rows show only one cylindrical hole each, while the squares in the remaining 12 rows each contain two cylindrical holes. For the squares containing two holes, one of the holes is always placed in the centre of the square, while the others are randomly placed in one of the square's corners. The depth and diameter of the holes vary between 0.3 and 8 mm (Figure 1).

The horizontal contrast axis (x-axis) represents the depth of the holes and the vertical contrast axis (y-axis) the diameter of the holes. The CDRAD analyser software calculates the image quality figure (IQF) which is an important parameter that describes the overall contrast detail visibility of the radiographic images. Low IQF values indicate better contrast resolution. The IQF is defined by the following equation (1) [18,22].

$$\mathrm{IQF} = \sum_{i=1}^{15} C_i \cdot D_{i,j} \qquad (1)$$

where $D_{i,j}$ denotes the threshold (j) diameter in contrast to columns i and C_i the correctly identified contrast values.

Usually, the inverse image quality figure (IQF_{inv}) is used to evaluate the quality of the radiographic images. The IQF_{inv} is defined by the following equation (2) [17,18,22], i.e. the higher the $IQF_{inv,}$ the better the image quality.

$$\mathrm{IQF_{inv}} = \frac{100}{\sum_{i=1}^{15} C_i \cdot D_{i,j}} \qquad (2)$$

2.3 Software

CDRAD image analyser software version 2.1.9 (Artinis medical systems B.V.) was used to calculate and automatically score the contrast detail resolution of the CDRAD radiographic images obtained with the different systems.

PCXMC version 2.0.1 Monte Carlo patient simulation software program (The Finnish Radiation and Nuclear Safety Authority (STUK), Helsinki, Finland) was used to calculate the effective doses (ED) of the patients.

2.4 Dosimeters

Piranha 657 (RTI Group, Mölndal, Sweden) is a solid-state dosimeter and was used to measure the entrance exposure to the patient. Thermo-luminescent dosimeters (TLD) detector type; MTS-N, Phosphor, LiF: Mg, Ti, (Batch number, RS1290/12, 30-003 Krakow Poland), were used to measure the absorbed organ doses of three organs. Five acquisitions were taken for the chest in both posterior-anterior (PA) and lateral (LAT) projections in chest examination protocol. In every acquisition, three TLD dosimeters were placed in the Alderson phantom, one TLD dosimeter was placed in the Thyroid gland area, and the other two were located in the right and left lung, respectively. The absorbed organ doses are the average values of these five measurements per organ. A TLD-reader, RadPro International GmbH, 42929 Wermelskirchen, Germany, was used to read the measured organ doses.

2.5 Clinical examination protocols

The radiation exposure to the patient and contrast detail resolution in chest and knee protocols for all three imaging modalities and their respective examination protocol settings were measured and

compared. The chest protocol was used for detecting low contrast details in order to diagnose lung diseases such as metastases or pneumothoraxes[23]. The knee protocol was used to diagnose the high contrast resolution of bone structures or fractures. The examination protocols and their respective dose level settings are shown in Table 1. The DR imaging systems consist of two different modalities, which are designated 'DR system 1' and 'DR system 2'.

It is possible to set the scan speed for all clinical applications of the MDSS imaging system between a speed of 1 and 8 seconds. The speed corresponds to the scan time, i.e. the higher the speed, the longer scan time and thus increased radiation exposure to the patient. Increasing the scan time from 4s to 8s results in approximately double radiation dose. In this study, the MDSS imaging system was set at different dose levels. These dose level settings are compared to the default settings of DR imaging systems. To achieve the highest dose level of MDSS imaging system, the dose level in MDSS imaging system of both chest and knee protocols was set to speed 8s. To investigate the best comparable contrast detail resolution for MDSS to the conventional DR X-ray imaging systems, the three dose levels have been set in the chest examination protocol. These dose levels are named as low dose level (speed 4s), medium dose level (speed 6s) and high dose level (speed 8s). However, there are only two dose level settings used in knee protocol, which are speed 6s and 8s.

2.6 Determination of radiation exposure to the patients

The measured entrance exposure was used to calculate and verify the Dose Area Product (DAP) of all X-ray imaging systems (Figure 2). 19 cm thick PMMA attenuation plates for chest protocol and 13 cm thick PMMA plates for knee protocol were placed on the wall stand detector to simulate the attenuation and scatter associated with patients of average adult size. A Piranha solid-state dosimeter, which is shielded against backscatter was placed on the PMMA blocks to measure the entrance exposure to the patients. In all imaging systems and all above-mentioned examination protocols, the entrance exposure (incident air kerma) was measured directly using the solid-state dosimeter. These measurements combined with the exposed area were used to verify the DAP values from the systems' DAP meters, using the following equation.

$$\mathrm{DAP} = \mathrm{A_{beam}} * \mathrm{D_{measured}}\ [\mathrm{mGycm^2}]\,, \qquad (3)$$

where the A_{beam} is the irradiated area, and $D_{measured}$ is the dose measured on the entrance surface of the patient (PMMA plates).

2.7 PCXMC simulations

The effective dose to the patient was calculated using the verified DAP values and simulated using the PCXMC software program. The effective dose was calculated according to the approach in the International Commission on Radiological Protection publication 103 (ICRP, 2007)[24]. It is not straightforward to use the PCXMC Monte Carlo algorithm to calculate the effective doses for the slot scanner based beam compared to the conventional X-ray exposure. Thus, the effective dose calculations in MDSS for the chest protocol were obtained using the method described by [25,26]. The

beam width and length are 400 mm x 0.5 mm and 360 mm x 0.5 mm for the chest PA and lateral projections respectively. The effective dose was calculated for each projection, and then these values are summed for all 800 simulations to give the total effective dose. The MDSS imaging system's nominal operating exposure parameters in the chest examination protocol, which were used as the input to the PCXMC software for simulating the effective doses to the patient are summarised in Table 2. As the dose to the knee is minimal, this method could not be applied for the calculation of effective dose in knee protocol. The calculated effective dose for the extremity (knee) is not sufficient for risk assessment of radiation dose to the patient. However, the effective dose estimation for the knee protocol in this study was used only for comparison purpose between the imaging systems. The absorbed dose to the lower leg bones (LLB) in the knee protocol was also determined.

2.8 Directly measured radiation exposure to the organs

The Alderson phantom (figure 3) was used to measure the organ doses directly from the lungs and thyroid. Five TLD dosimeters were exposed per organ. The TLD dosimeters for the lungs were placed on symmetrical sides of the chest area in the Alderson phantom, which is slice 15 on the phantom height. The TLD dosimeters were placed in the lung area according to the instructions of the Alderson phantom and as same as described by Cakmak et al [27]. The locations of the TLD dosimeters on the Alderson phantom are illustrated in Figure 3. In the MDSS imaging system, the TLD dosimeters were also exposed in the preview (scout) acquisition modes in both projections (PA and lateral).

The directly measured organ doses were also compared to the simulated organ doses. The difference between the measured and the simulated organ doses was calculated using the following formula:

$$\frac{D_m - D_c}{D_m} \cdot 100\% \qquad (4)$$

where the D_m is the measured organ dose, and D_c is the calculated organ dose.

2.9 Contrast derail resolution measurement

The CDRAD test object was sandwiched between the PMMA attenuation blocks. The CDRAD test object and PMMA attenuation blocks were centred in the middle of the X-ray beam. Ten images of the phantom were acquired for each protocol. The contrast detail resolution measurement setup is illustrated in Figure 4.

2.10 Evaluation of contrast detail resolution

To evaluate the image quality of all systems objectively for the chest and knee protocols, the CDRAD analyser software package was used to score the acquired images of the CDRAD test object automatically. The CDRAD analyser software requires a minimum of ten input images acquired using the same radiographic factors to produce one contrast detail curve. CDRAD phantom images in DICOM format were sent to a PACS station or collected directly from the imaging modality. The CDRAD analyser software was used to automatically determine the IQF and IQF_{inv}, contrast detail curves (CDC) and percentage detected of the CDRAD phantom. The percentage of the total detected

(%) of the CDRAD image is the ratio of correctly identified hole-positions to the total number of squares of the CDRAD test object. The correct observed ratio is calculated as in equation 4[28,29] .

$$\text{Correct observation ratio} = \frac{\text{Correct observations}}{\text{Total number of squares}} \cdot 100\% \quad (4)$$

2.11 System settings

The differences between the default parameter (exposure parameter) settings of the three imaging systems are source image distance (SID), tube voltage (kV), additional filtration and other relevant parameters in both clinical examination protocols (chest and knee). These differences are summarised in Table 3 and 4. An anti-scatter grid was used on the chest protocol of both DR systems, whereas the MDSS images were acquired without an anti-scatter grid. In addition, none of the imaging systems used an anti-scatter grid for the knee protocol.

3. RESULTS

3.1 Verification of DAP values

The DAP meters outputs were tested for all protocols, the maximum deviation between the displayed and calculated DAP values was 8.5%, which was within a tolerance of ± 25%[30,31] .

3.2 Organ dose measurement

The directly measured organ doses in the chest protocol for all imaging systems and their respective settings are summarised in Table 5. The measured doses in the left lungs are higher than the doses measured in the right lungs, as the left lungs are closer to the X-ray source in the lateral projection. Both DR systems have higher organ doses compared to the organ doses of MDSS imaging systems for all speeds. The DR system 2 has the highest organ doses. Organ doses for the MDSS systems approximately increase in proportion with the selected speed. The organ doses of MDSS speed 8s should be approximately double as high as the organ doses of MDSS speed 4s.There are several factors including measurements uncertainty, uncertainties related to the TLD dosimeters and reading uncertainty, which may explain some of the inconsistencies between the dose level settings (speeds) and organ doses. There were also differences between the phantom and calculated values, which is due to a difference in size between the physical and the virtual phantoms. Figure 5 shows a comparison between the average of the measured organ doses and simulated organ doses in chest examination protocol for all imaging systems.

3.3 Calculated effective doses

The calculated effective dose (ED) in chest protocols for all imaging systems are given in Table 6. The DAP values from the systems were used to calculate the effective doses (ED). The corresponding calculated ED results for the knee protocol of all imaging modalities are summarised in Table 7. The calculated effective doses for both chest and knee examination protocols is less for all of the dose levels of the MDSS imaging system compared to DR imaging systems. The percentage difference in effective dose between the MDSS settings (speed 4s, speed 6s and speed 8s) and DR imaging systems in both chest and knee protocols are summarised in Table 9. Figure 6 (a and b) illustrates a comparison overview of the calculated effective doses on both chest and knee protocols for all imaging systems. The total calculated effective doses of all dose level settings for the MDSS included both the preview (scout) mode and the primary exposure. The comparison of calculated absorbed organ doses to the lower leg bones (LLB) in knee protocol for all imaging systems are illustrated in Figure 6 (c). The DR systems 1 exposes the highest dose to the LLB and MDSS speed 6s has the lowest dose to LLB, which corresponds to the effective dose in knee protocol.

3.4 Image quality figure (IQF) and contrast detail resolution

The IQF, IQF_{inv} and total detected percentage of the CDRAD phantom images in both chest and knee protocols are given in Table 8. CDRAD analyser software calculates the IQF and IQF_{inv} parameters automatically. The percentage detected is the percentage of the detected hole-diameter and hole-depth of the images. The IQF_{inv} for the chest and knee protocols for all imaging systems is shown in Figure 7.

In order to produce a contrast detail curve, the depth of the CDRAD phantom thinnest visible holes is plotted against the hole diameter. To compare the contrast detail resolution of all imaging systems, the contrast detail curves are plotted in the same coordinate system and given in Figures 8 and 9, which are for chest and knee protocols respectively. The more the curve is located at the lower left side of the coordinate system the better contrast resolution has the imaging system. According to the contrast detail curves of the chest examination protocol shown in Figure 8, the DR System 2 and MDSS high-dose protocol settings (speed 8s.) have the best contrast detail resolutions. The DR system 1 is slightly better for the small hole-diameters of the phantom, where the MDSS speed 8s is the best for the large hole-diameters in the chest protocol. The overall IQF_{inv} of MDSS speed 8s is 2.72, whereas the total IQF_{inv} of DR system 1 is 2.59. The DR system 2 and MDSS speed 6s has the same image contrast resolution. The IQF_{inv} of DR system 2 and MDS speed 6s are 2.51 and 2.48 respectively.

The corresponding contrast detail curves of knee protocol for all imaging systems are plotted in the same coordinate system and shown in Figure 9. Imaging systems DR system 1 and MDSS speed 8s has the highest scored overall IQF_{inv} in knee protocol. The IQF_{inv} of DR system 1 and MDS speed 8s are 3.37 and 3.20 respectively.

4. DISCUSSION

There was wide variation between the settings of the exposure parameters of the imaging systems used in this study. The SID, tube voltage, filtration and exposure mode are different in the clinical setting for the imaging systems. However, both image quality (contrast detail resolution) and radiation exposure to the patients in all imaging systems and dose level settings were broadly comparable.

4.1 Patient dose

According to the measured absorbed organ doses from chest protocol imaging shown in Table 5, the default setting (speed 4s) in the MDSS imaging system gave the least absorbed dose to the patient compared to all other systems and settings, while the DR system 1 exposes the highest organ dose and effective dose (Table 6) to the patients. The thyroid is located outside the direct radiation beam and was exposed only to the scattered radiation; therefore, the absorbed doses for thyroid are lower than the absorbed doses for the lungs. There is a difference between the directly measured organ doses and the simulated organ doses. The average of directly measured absorbed lung doses were between 17% and 30% higher than the simulated lung absorbed organ doses. However, the difference between the calculated and measured organ doses to the thyroid ranges 17% to 25%. This difference applies to all imaging systems and settings in the chest protocol. The PCXMC software calculates the dose to the lungs as a whole rather than separately. Therefore we have average the measured lung doses for the right and left lungs. The calculated (simulated) doses of both lungs correspond roughly to the directly measured dose to the right lung. The directly measured doses to the left lung are higher than the directly measured doses to the right lung because the left lung is closer to the X-ray source in the LAT acquisition.

The measured organ doses in MDSS imaging system for both chest and knee protocols are less than the measured organ doses in DR imaging systems. However, the default setting (speed 4s) exposes the minimum radiation to the measured organs. In general, the DR system 1 exposes the patient to the highest radiation doses in both chest and knee clinical examination protocols. The measured organ doses in DR system 1 are also the highest compared to the other imaging systems and settings.

4.2 Chest protocol

The highest dose level setting (speed 8s) of MDSS imaging system for chest protocol was shown to have the highest IQF_{inv} values. On the other hand, the medium dose level setting of MDSS (speed 6s) and DR-system 2 in chest protocol have the same $IQF_{inv.}$ The default setting of MDSS (speed 4s) acquisition had the lowest IQF_{inv} for the chest protocol. These results indicate that speed 4s of the MDSS would be inferior in terms of image quality compared to the DR systems but that speed 6s or 8s may be suitable, but with the advantage of a lower patient dose. The ED dose reduction compared to the DR systems was up to 17.6%, 42.6% and 60% lower for the speed 8s speed 6s and speed 4s respectively of the MDSS system.

4.3 Knee protocol

The DR system 1 had the best contrast detail resolution for the knee protocol, whereas the MDSS speed 8s had the second best contrast resolution and provided better IQF_{inv} than the DR system 2. The default (speed 6s) for the MDSS had an inferior image quality compared to the DR systems, but the higher dose (speed 8s) may be acceptable for imaging of the knee. The ED dose in the default MDSS knee protocol setting (speed 6s) was between 47% to 51% lower than for DR imaging systems, while the high level dose setting of MDSS (speed 8s) ranged between 29% and 35% lower than the DR imaging systems. The absorbed organ dose lower leg reduction compared to the DR systems was up to 24% and 51% lower for the speed 8s and 6s respectively of the MDSS system.

4.4 Comparison of the systems

The image quality and effective dose to the patient for two conventional DR systems in clinical use were assessed for comparison. There is no consensus on the optimal imaging conditions for a chest x-ray, but often images are acquired with 125kV and an anti-scatter grid. The DR systems in this study used a tube voltage higher than 125kV for chest imaging. The exposure parameters of these systems may not necessarily be optimally adjusted, but the images were considered clinically acceptable. It is possible that another DR system may be better than the two DR system in this study. The overall assessment of the results achieved in both image quality measurement and determined radiation exposure to the patients of the systems in both chest and extremity protocols indicates that the MDSS imaging system has the potential to provide sufficient diagnostic information and at the same time save patient doses compared to conventional DR X-ray systems. Additional clinical and technical studies and comprehensive clinical audit should be carried out to test if the MDSS X-ray imaging system can be used for diagnostic purposes. The advantage of this study is that the results obtained in image quality are based on an objective assessment, which is independent of a subjective assessment of observer scoring.

5. CONCLUSIONS

The contrast detail resolution of the MDSS high and medium dose levels (speed 6s and 8s) settings in chest examination protocol have been found to be equal to or higher than the contrast detail resolution of both DR imaging systems. The contrast detail resolution of the MDSS high-level dose (speed 8s) setting in knee examination protocol is the same as or higher than the contrast detail resolution of DR imaging systems. At MDSS speed 8s in knee protocol and speed 6s in chest protocol, there is a potent dose saving without compromising the image contrast. If the MDSS imaging system is operated at these higher dose levels, then it has potential to be used for more than quantifying leg length or scoliosis and may be usable for a broader range of imaging including diagnostics.

6. REFERENCES

1. Sigurdson AJ, Bhatti P, et al. Routine diagnostic X-ray examinations and increased frequency of chromosome translocations among U.S. radiologic technologists. *Cancer Res.* 2009;68(21):8825-8831. doi:10.1158/0008-5472.CAN-08-1691.

2. Rasuli B, Ghorbani M, Juybari RT. Radiation dose measurement for patients undergoing common spine medical x-ray examinations and proposed local diagnostic reference levels. *Radiation Measurements*. 2016;87:29-34. doi:10.1016/j.radmeas.2016.02.017.

3. Lazennec JY, Rousseau MA, Rangel A, et al. Pelvis and total hip arthroplasty acetabular component orientations in sitting and standing positions: Measurements reproducibility with EOS imaging system versus conventional radiographies. *Orthopaedics and Traumatology: Surgery and Research*. 2011;97(4):373-380. doi:10.1016/j.otsr.2011.02.006.

4. Dubousset J, Charpak G, Dorion I, et al. A new 2D and 3D imaging approach to musculoskeletal physiology and pathology with low-dose radiation and the standing position: the EOS system. *Bulletin de l'Academie nationale de medecine*. 2005;189(2):287—97; discussion 297—300. http://europepmc.org/abstract/MED/16114859.

5. Rehm J, Germann T, Akbar M, et al. 3D-modeling of the spine using EOS imaging system: Inter-reader reproducibility and reliability. *PLoS ONE*. 2017;12(2):1-13. doi:10.1371/journal.pone.0171258.

6. Lazennec J-Y, Rousseau M-A, Brusson A, et al. Total Hip prostheses in standing, sitting and squatting positions: An overview of our 8 years practice using the EOS imaging technology. *The Open Orthopaedics Journal*. 2015;9(1):26-44. doi:10.2174/1874325001509010026.

7. Hui SCN, Chu WCW. Supplementary addendum to radiation dose of digital radiography (DR) versus micro-dose x-ray (EOS) on patients with adolescent idiopathic scoliosis. *Scoliosis and Spinal Disorders*. 2018;13(1):1-8. doi:10.1186/s13013-017-0148-5.

8. Jensen J, Mussmann BR, Hjarbæk J, et al. Microdose acquisition in adolescent leg length discrepancy using a low-dose biplane imaging system. *Acta Radiologica*. 2017;58(9):1108-1114. doi:10.1177/0284185116682381.

9. Newton PO, Khandwala Y, Bartley CE, Reighard FG, Bastrom TP, Yaszay B. New EOS imaging protocol allows a substantial reduction in radiation exposure for scoliosis patients. *Spine Deformity*. 2016;4(2):138-144. doi:10.1016/j.jspd.2015.09.002.

10. Bittersohl B, Freitas J, Zaps D, et al. The orthopaedic forum : EOS imaging of the human pelvis: Reliability, validity, and controlled comparison with radiography. *Journal of Bone and Joint Surgery - Series A*. 2013;95(9):1-9. doi:10.2106/JBJS.K.01591.

11. McKenna C, Wade R, Faria R, et al. EOS 2D/3D X-ray imaging system: a systematic review

and economic evaluation. *Health technology assessment (Winchester, England)*. 2012;16(14):1-188. doi:10.3310/hta16140.

12. Deschênes S, Charron G, Beaudoin G, et al. Diagnostic imaging of spinal deformities: reducing patients radiation dose with a new slot-scanning X-ray imager. *Spine*. 2010;35(9):989-994. doi:10.1097/BRS.0b013e3181bdcaa4.

13. Melhem E, Assi A, El Rachkidi R, Ghanem I. EOS®biplanar X-ray imaging: concept, developments, benefits, and limitations. *Journal of Children's Orthopaedics*. 2016;10(1):1-14. doi:10.1007/s11832-016-0713-0.

14. Damet J, Fournier P, Monnin P, et al. Occupational and patient exposure as well as image quality for full spine examinations with the EOS imaging system. *Medical Physics*. 2014;41(6Part1):063901. doi:10.1118/1.4873333.

15. The EOS 2D / 3D imaging system: NICE diagnostics guidance 1. 2011: 1-27. www.nice.org.uk/dg1

16. Alsleem H, U P, Mong KS, Davidson R. Effects of radiographic techniques on the low-contrast detail detectability performance of digital radiography systems. *Radiologic Technology*. 2014;85(6):614-622. doi:10.1118/1.2868780.

17. Geso M, Shanahan M, Alghamdi SS, Davidson R, Alghamdi S. Low-contrast detail phantom: Proof of concept. *Journal of Medical Imaging and Radiation Sciences*. 2016;47(1):60-65. doi:10.1016/j.jmir.2015.11.001.

18. Pascoal A, Lawinski CP, Honey I, Blake P. Evaluation of a software package for automated quality assessment of contrast detail images--comparison with subjective visual assessment. *Physics in medicine and biology*. 2005;50(23):5743-5757. doi:10.1088/0031-9155/50/23/023.

19. Illes T, Somoskeoy S. The EOS™ imaging system and its uses in daily orthopaedic practice. *International Orthopaedics*. 2012;36(7):1325-1331. doi:10.1007/s00264-012-1512-y.

20. Vano E, Gonzalez L, Fernandez JM, Prieto C, Guibelalde E. Influence of patient thickness and operation modes on occupational and patient radiation doses in interventional cardiology. *Radiation Protection Dosimetry*. 2006;118(3):325-330. doi:10.1093/rpd/nci369.

21. Ubeda C, Vano E, Gonzalez L, et al. Scatter and staff dose levels in paediatric interventional cardiology: A multicentre study. *Radiation Protection Dosimetry*. 2010;140(1):67-74. doi:10.1093/rpd/ncq039.

22. Mourik JEM, Van Der Tol P. Comparison of wireless detectors for digital radiography systems: Image quality and dose. *Radiation Protection Dosimetry*. 2016;169(1):303-307.

23. McEntee M, Frawley H, Brennan PC. A comparison of low contrast performance for amorphous Silicon / caesium iodide direct radiography with a computed radiography : A contrast detail phantom study. *Radiography*. 2007;13, 89-94. doi:10.1016/j.radi.2006.01.004.

24. Holm LE, Cox R,Pan ZQ. et al.The 2007 recommendations ICRP Publication 103 . 2007. https://doi.org/10.1016/j.icrp.2007.10.003

25. Law M, Ma W-K, Lau D, et al. Cumulative effective dose and cancer risk for pediatric population in repetitive full spine follow-up imaging: How micro dose is the EOS microdose protocol? *European Journal of Radiology*. 2018;101(February):87-91. doi:10.1016/j.ejrad.2018.02.015.

26. Law M, Ma WK, Chan E, et al. Evaluation of cumulative effective dose and cancer risk from repetitive full spine imaging using EOS system: Impact to adolescent patients of different populations. *European Journal of Radiology*. 2017;96(July):1-5. doi:10.1016/j.ejrad.2017.09.006.

27. Cakmak ED, Tuncel N, Sindir B. Assessment of organ dose by direct and indirect measurements for a wide bore X-ray Computed Tomography unit that used in radiotherapy. *International Journal of Medical Physics*. 2015;(May):132-142. doi:10.4236/ijmpcero.2015.42017.

28. Thomas JA, Chakrabarti K, Kaczmarek R, Romanyukha A. Contrast-detail phantom scoring methodology. *Medical physics*. 2005;32:807-814. doi:10.1118/1.1862097.

29. Aksoy ME, Kamasak ME, Akkur E, Ucgul A, Basak M, Alaca H. Evaluation and comparison of image quality for indirect flat panel systems with CsI and GOS scintillators. *2012 7th International Symposium on Health Informatics and Bioinformatics, HIBIT 2012*. 2012:57-62. doi:10.1109/HIBIT.2012.6209043.

30. *Radiation protection report N ° 162: Criteria for acceptability of medical radiological equipment used in diagnostic radiology, nuclear medicine and radiotherapy*. 2012. doi:10.2768/22561.

31. International Electrotechnical Commission (IEC): IEC 60580 Ed 2.0: Medical Electrical Equipment - Dose area product meters. Geneva. 2000 IEC. https://webstore.iec.ch/publication/2516&preview=1

7. LIST OF FIGURES:

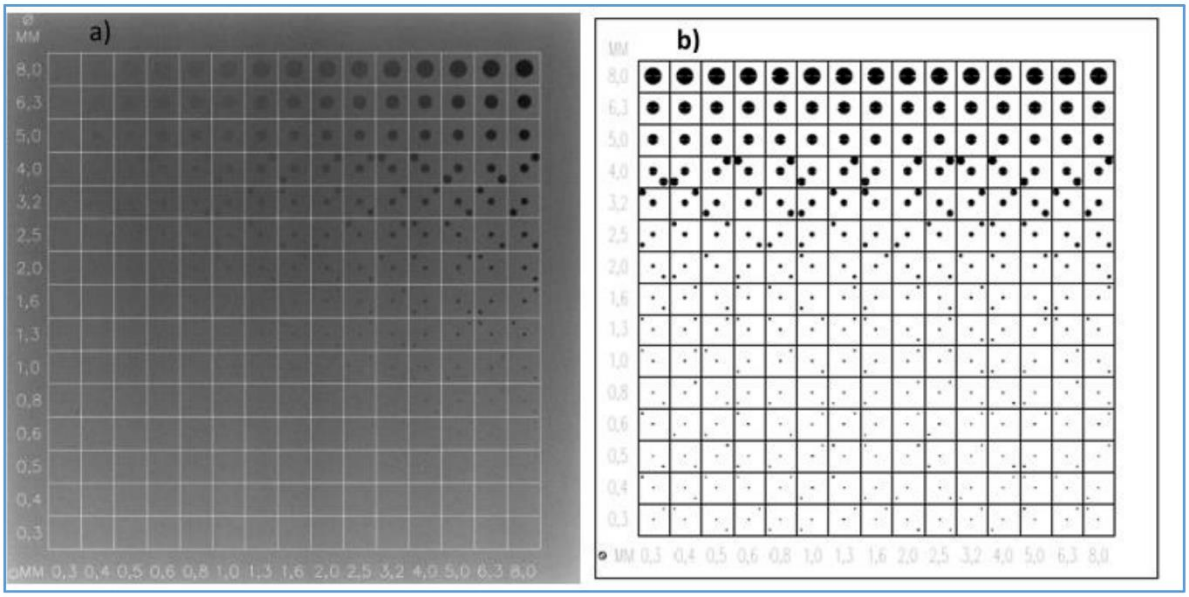

Figure 1: a) Radiographic image of the CDRAD test object containing 225 details patterns. b). Visual illustration of the CDRAD test object composed of PMMA attenuation plate with holes (CDRAD test object user manual).

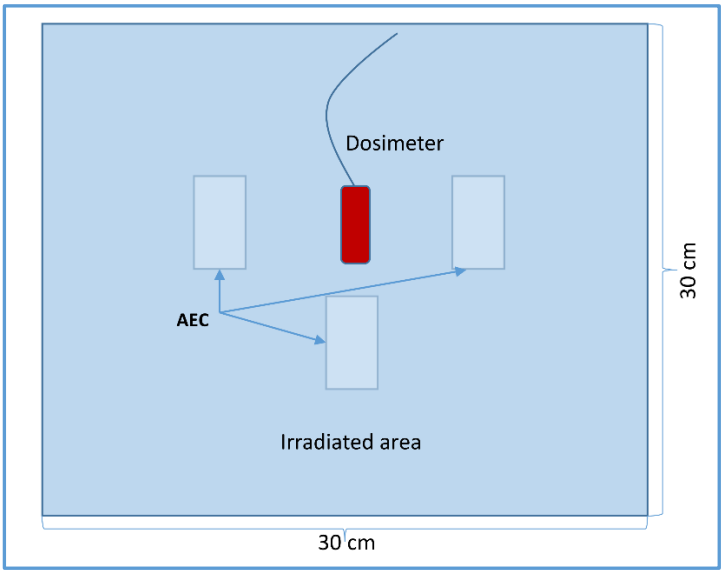

Figure 2: DAP verification setup with the irradiated area and solid-state dosimeter placed in the centre of the radiation beam for DR imaging systems, AEC = Automatic exposure control.

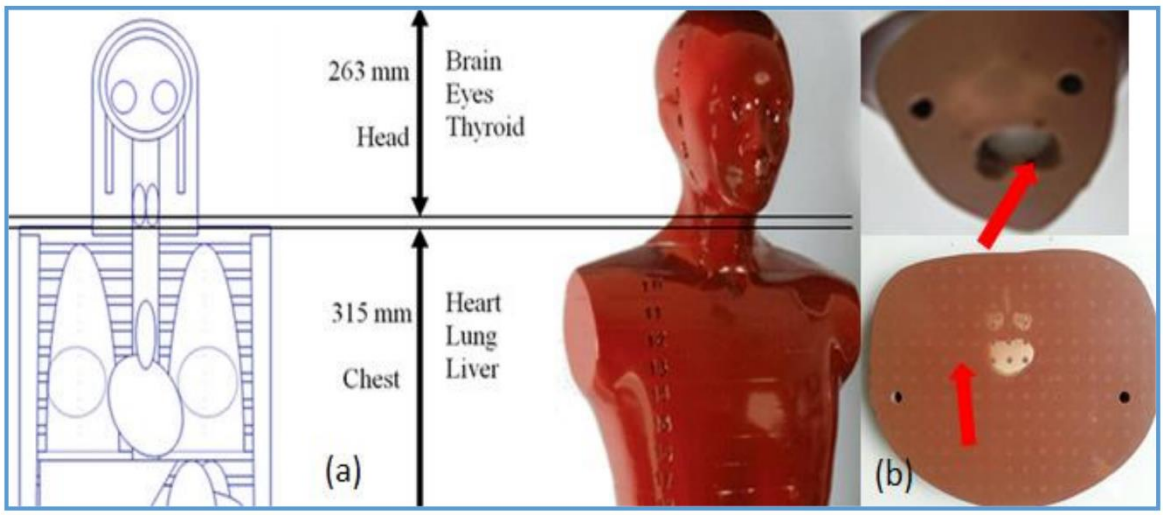

Figure 3: Dose measurement setup on Alderson phantom, (a) Alderson phantom with organ overview (b) positioning of dosimeters for Lung dose and Thyroid dose measurement indicated with arrows.

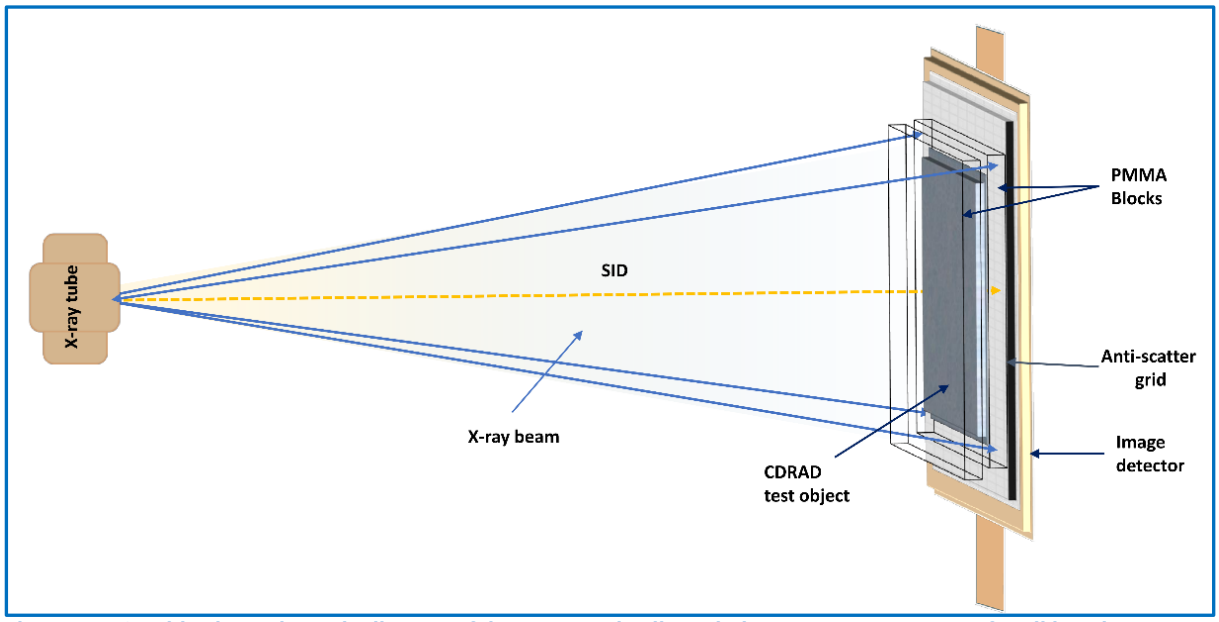

Figure 4: A 3D side view schematic diagram of the contrast detail resolution measurement setup for all imaging systems and settings, SID = source to image distance.

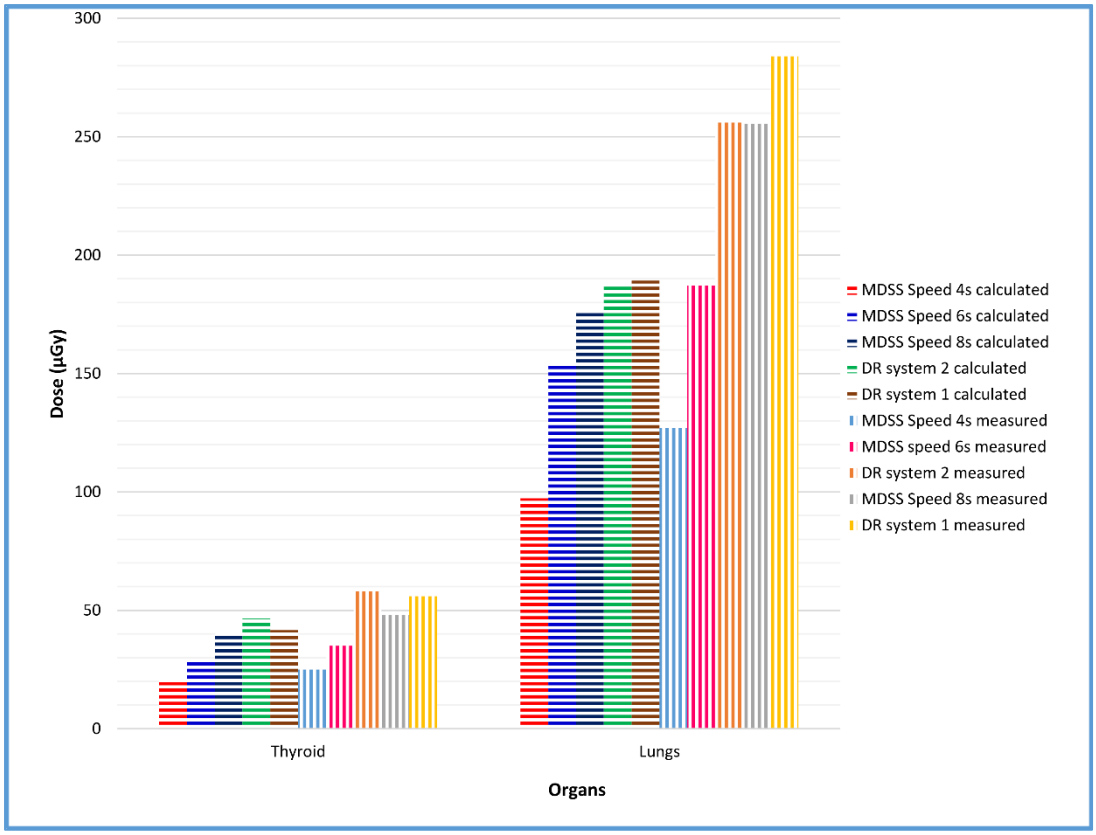

Figure 5: Comparison between the average of the measured absorbed organ doses and simulated absorbed doses in chest protocol for all imaging systems.

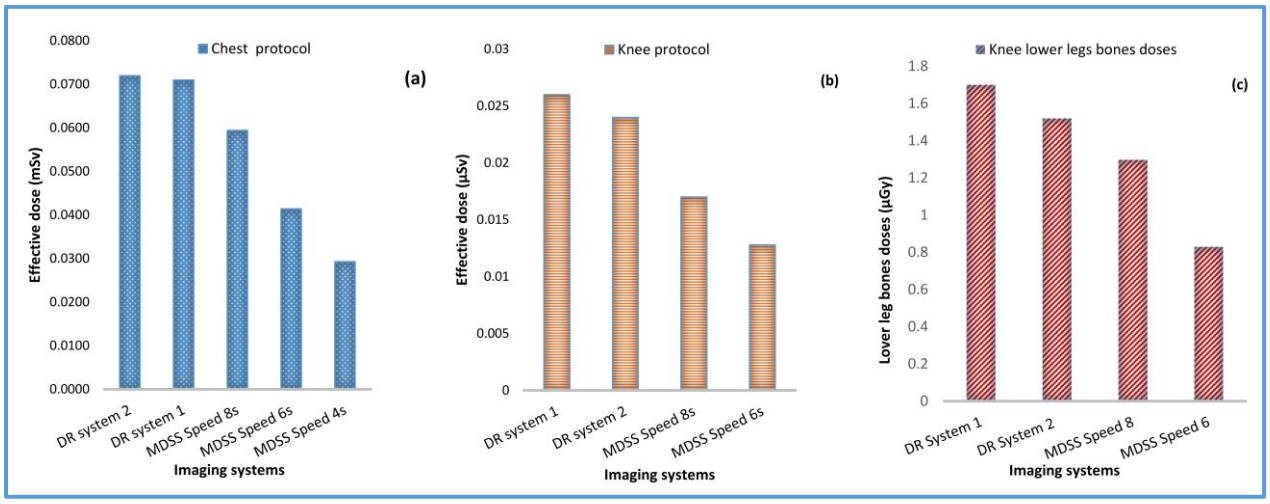

Figure 6: Comparison between effective doses in (a) chest protocol for all imaging systems. (b) knee protocol for all imaging systems and (c) lower leg organ dose (LLB OD) for all imaging systems in knee protocol.

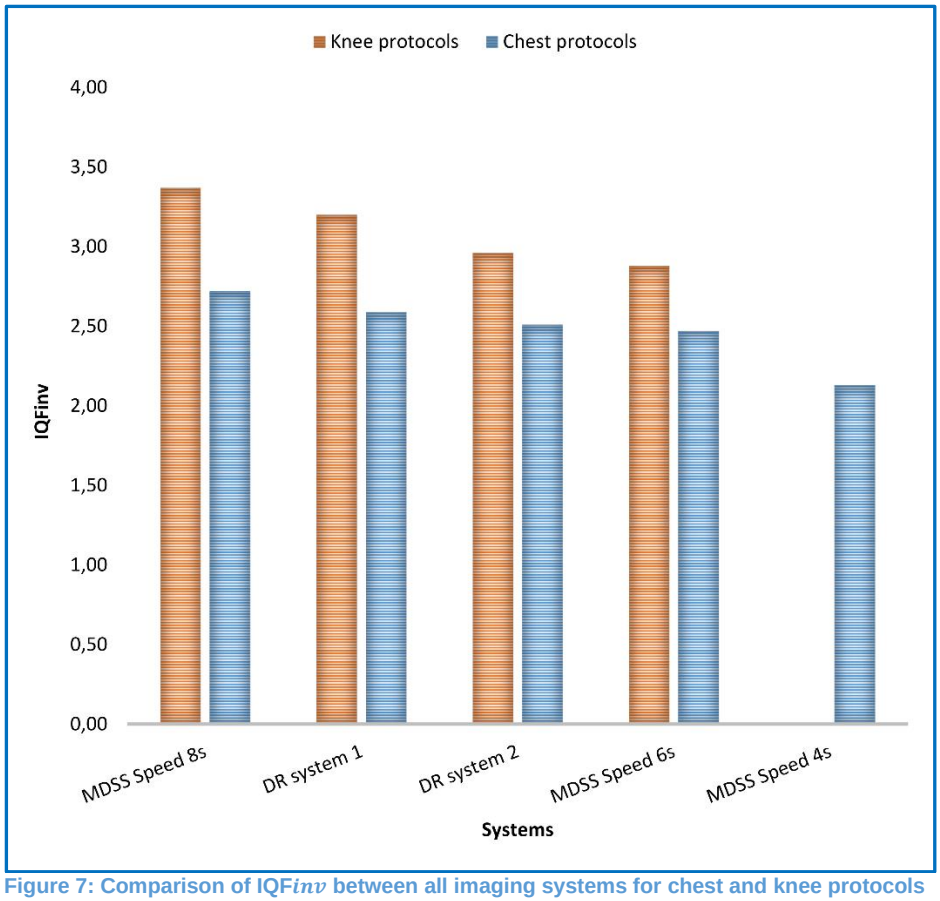

Figure 7: Comparison of IQFinv between all imaging systems for chest and knee protocols

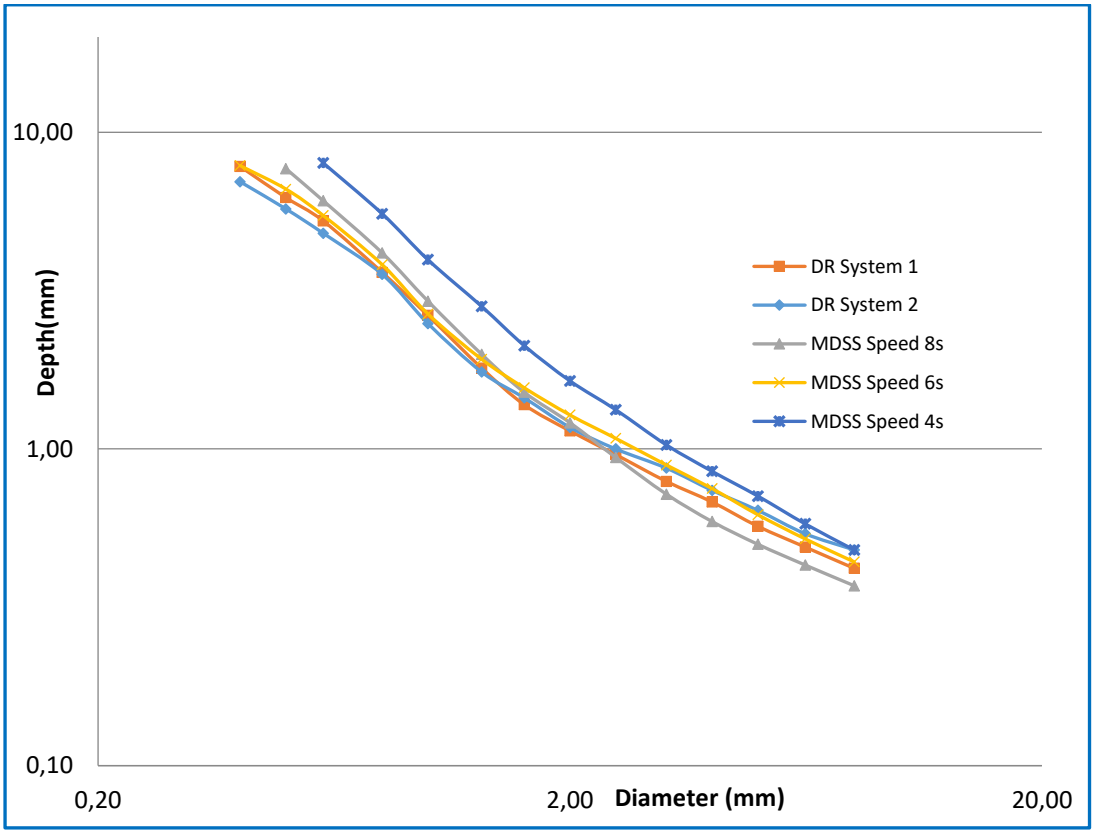

Figure 8: The contrast detail curves in chest protocol for all imaging systems

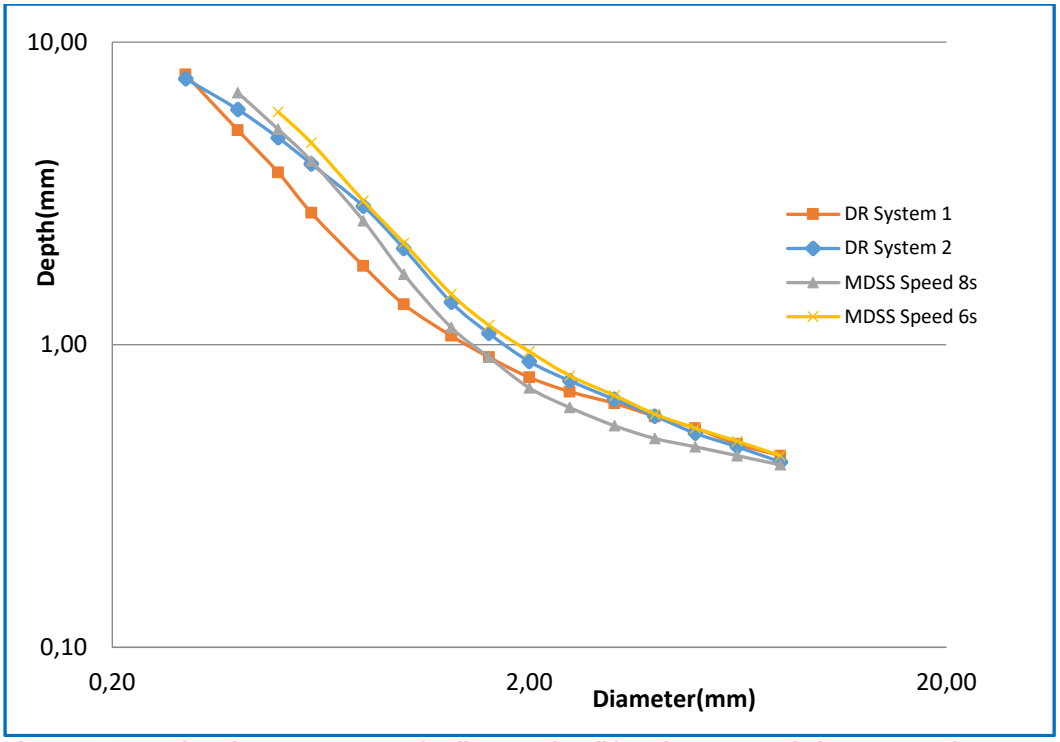

Figure 9: Comparison between contrast detail curves for all imaging systems in knee protocol.

8. ACKNOWLEDGEMENTS

We appreciate the help of the Clinical Engineering Department at the Southern Region of Denmark for their valuable support, providing most of the equipment used in this study including phantoms, dosimeters and software. We are grateful for the use of the X-ray equipment in the Radiology Department at the Odense University Hospital. We also acknowledge the support of the EUTEMPE-RX module 7, 'Optimisation of X-ray imaging using standard and innovative techniques' in the development of the research ideas and plan.